International Journal of Nanoelectronics and Materials
Volume 14 (Special Issue) August 2021 [225-240]

Effect of the Different Printing Patterns of Graphene Nanoparticles in Conductive Ink on Electrical and Mechanical Performance

Adzni Md. Saad[1,2], Mohd Azli Salim[1,2,3*], Mohammed Hussin A. Al-Mola[4], Fauzi Ahmad[1], Hartini Saad[5] and Mohd Zaid Akop

[1]Fakulti Kejuruteraan Mekanikal, Universiti Teknikal Malaysia Melaka, Hang Tuah Jaya, 76100 Durian Tunggal, Melaka, Malaysia
[2]Advanced Manufacturing Centre, Universiti Teknikal Malaysia Melaka, Hang Tuah Jaya, 76100 Durian Tungggal, Melaka, Malaysia
[3]Intelligent Engineering Technology Services Sdn. Bhd., No.1, Jalan TU43, Taman Tasik Utama, 76450 Ayer Keroh, Melaka, Malaysia
[4]Faculty of Petroleum and Mining Engineering, University of Mosul, Mosul, Iraq.
[5]Jabatan Kejuruteraan, Sekolah Kejuruteraan dan Sains Kreatif, Kolej Yayasan Pelajaran Johor, Jalan Kulai – Kota Tinggi, KM 16, Jalan Kulai, 81000 Johor, Malaysia

ABSTRACT

The utilization of graphene in the formation of conductive ink has been positively accepted by the electronics industry especially with the emerging of printable and flexible electronics. Because of that, it motivates this study to investigate the electrical, mechanical, and morphological properties for different patterns of Graphene Nanoparticle (GNP) conductive ink. The samples were prepared using the screen-printing technique with a low annealing temperature of 100 ºC for 30 minutes. The investigated parameter for the electrical property was the sheet resistivity, which showed that the zigzag pattern recorded the highest value of 1.077 kΩ/sq at the 3 mm of ink thickness. For the mechanical properties, the highest of hardness for 2 mm thickness was the curve pattern and for 3 mm was the square pattern, with the values of 3.849 GPa and 4.913 GPa. Both maximum values showed a direct correlation with the behavior of the elastic modulus of the ink. The maximum values of elastic modulus were recorded at the same ink pattern and thickness. For the morphological analysis, the surface roughness and qualitative analysis using SEM images were performed. The surface roughness showed that the increase of GNP in the composition increased the surface roughness because it decreased the homogeneity of the mixture. The recorded SEM images of the ink layer microstructure surface showed a direct correlation with the obtained sheet resistivity data. The samples that produced high sheet resistivity showed the presence of bumps, creases, and defects on the ink layer surface. Based on the obtained data, the correlation between electrical, mechanical, and morphological properties can be established for the GNP conductive ink with various patterns and thicknesses.

Keywords: Graphene nanoparticles, conductive ink, sheet resistivity, nanoindentation, morphology analysis

1. INTRODUCTION

Conductive ink has become increasingly popular in recent years due to its capability to become an alternative approach to constructing electric circuitry. With the growth of printable and flexible electronics, the utilization of conductive has become more important [1]. The main prominent advantages of conductive ink are its compatibility and producibility [2]. Many researchers have shown that conductive ink can be applied to various applications and can be produced using different types of production techniques. Some of the attractive applications of conductive ink are in the field of automotive monitoring systems and neurosciences [3,4]. The

*Corresponding Author: azli@utem.edu.my

challenge of producing conductive ink is to obtain the appropriate material and suitable printing technique for a specific application.

The process of printing the conductive ink pattern requires the formation of a fine line, which requires the utilization of nanoparticles in the material. Because of that, silver nanoparticles have been most extensively used because of their high electrical conductivity and oxidation stability. The introduction of graphene also provides more opportunities for technological advancement in this field. It has comparable electrical conductivity performance as silver and is considered a zero-gap semiconductor material [5]. Furthermore, graphene has better chemical stability and mechanical properties as compared to other metallic-based material [6]. It also possesses large electron mobility at room temperature and smaller resistivity than silver [7]. Because of that, this study utilizes graphene as the filler material for the composition of the conductive ink.

In terms of the method of producing the ink pattern, various approaches have been introduced. Some of the most popular techniques are screen printing, gravure printing, inkjet printing, and 3D printing [8,9]. Each of these techniques has its own advantages and superior characteristics. This study employs screen printing as the method to print the ink pattern. It is because, this method is considered the most versatile and mature technique, which is simpler and faster as compared to other printing tools. The patterns can also be easily reproduced by repeating the process on the new substrates with an optimal operating procedure [8]. It also has the capability to produce a thick film in a single pass that reduces the processing time [10].

The performance of the conductive ink is mainly measured by its electrical properties, especially the ability of the ink to conduct electricity. Because of that, sheet resistivity analysis is generally performed for the thin film [11]. For this study, additional properties are also measured, which are the mechanical and microstructure properties. The investigated mechanical properties include the hardness, elastic modulus, maximum applied force, and penetration by using the nanoindentation technique. It can reveal the material response to the external disturbance [12]. For the microstructure properties, quantitative analysis is performed by determining the surface roughness [13]. The scanning electron microscopy (SEM) images are obtained to perform the qualitative analysis.

2. MATERIAL AND METHODS

2.1 Sample Preparation

Conductive ink requires a certain procedure of producing the workable samples. It includes the formulation of the ink, printing the ink on the substrate, and curing the ink. All these steps must be performed appropriately to ensure the produced samples can be used to investigate the determined parameters.

2.1.1 Conductive Ink Formulation

The main components of material to formulate the conductive ink are the filler, binder, and hardener. The filler is the component that produces the ability of the ink to conduct electricity. Binder is used to unifying all the formulation components together and a hardener is used to transform the ink from liquid-state to become ink paste [14]. For this study, Graphene Nanoparticles (GNP) with a specific surface area of 500 m^2/g and a molecular mass of 12.01 g/mol were used as the filler, which were obtained from Sigma Aldrich. Bisphenol-A diglycidyl (DGEBA) ethers epoxy resin was used as the binder and The Hunstman polyetheramine D230 was used as a hardener. The conductive ink formulation used for this study was referred to the

previous research work by Mokhlis [15]. Based on this work, the formulation of GNP conductive ink was performed using filler loading starting from 10 %wt up to 35 %wt with the 5 %wt increment. The best formulation was chosen for this study and it is shown in Table 1 below. The enhancement of electrical conductivity performance is relying on the formation of the conductive path in the composition. Because of that, the higher filler content contributes to better electrical performance [8]. But it is also necessary to consider the cost of formulating conductive ink to have comparable performance. This was done by a previous researcher by obtaining the least amount GNP filler requires to have similar performance [16]. Then, the materials were mixed according to individual weight by using a thixy mixer at the speed of 3,000 rpm for 3 minutes.

Table 1 Formulation of GNP conductive ink

Filler		Binder		Hardener	Total
(wt.%)	(g)	(wt.%)	(g)	(g)	(g)
35	0.7	65	1.3	0.39	2.39

2.1.2 Printing Method

Manual screen-printing was used to produce the patterns of the GNP ink. It is because this technique is suitable to print ink thick patterns on various types of ink especially with low resistivity [17]. Thermoplastic polyurethane (TPU) was chosen as the substrate because it possesses the stretchability characteristic that is required for this study. TPU can withstand a high-temperature process and recover the rubber-like property during solidification [18]. The ink was printed using the stencil in four different patterns, which are straight-line, curve, square and zigzag. These patterns are the most used electrical circuitry, especially in microelectronics applications. Each of the patterns was printed in 3 different ink thicknesses. The detailed geometry of the patterns is illustrated in Figure 1 below.

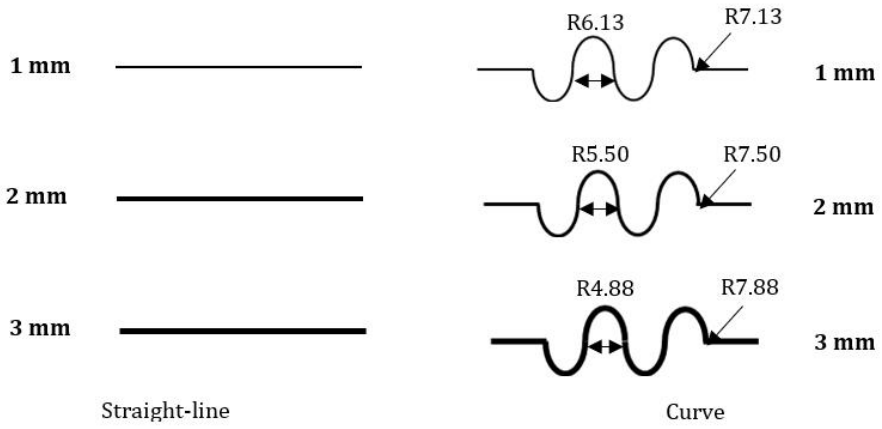

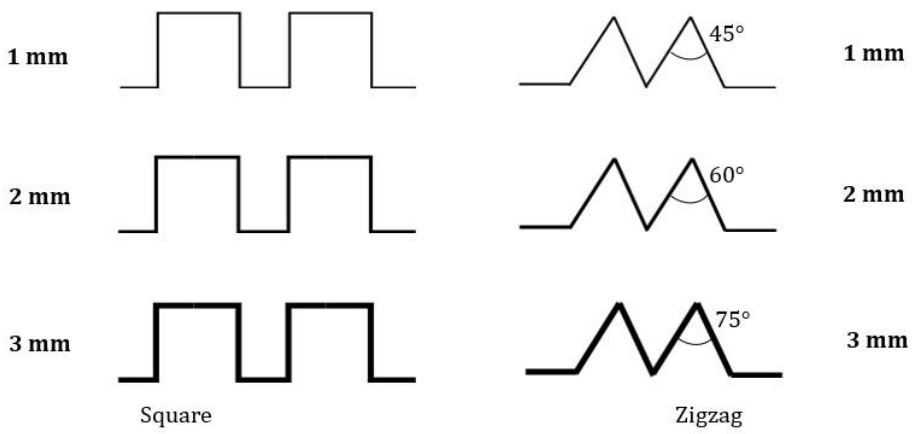

Figure 1. Conductive ink test patterns.

2.1.3 Curing Process

The curing process is a post-treatment that was performed on the ink samples by using heat. For this study, universal oven UF55 was used to cure the samples at a low temperature of 100 °C for 30 minutes. The purpose of the curing process is to anneal the composition by removing the excess solvent and encouraging the chemical reaction to occur to form the conductive network paths. It can also enhance the adhesion of GNP inks to the TPU substrate [19]. Then, the samples were dried at room temperature.

2.2 Sample Characterization

The characterization procedure was carried out for all four types of patterns. The purpose is to obtain data in investigating the electrical, mechanical, and microstructure properties of the samples. The measurement points on the samples were precisely determined to ensure the consistency of the data and it is shown in Figure 2 below. There are 3 measurement points for each of the samples. By having consistent data, it validates the investigation of discovering the correlation between each of the examined parameters.

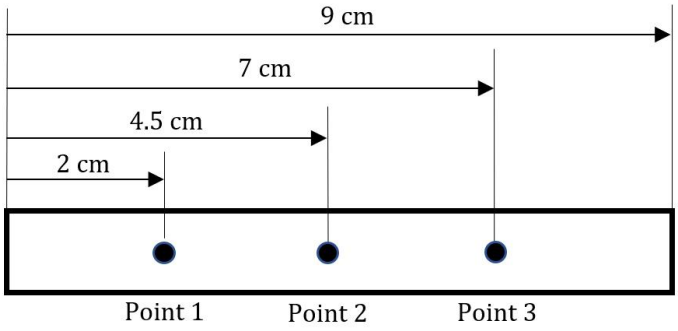

Figure 2. Measurement points on the sample.

2.2.1. Electrical Properties

For this study, the obtained parameter to investigate the electrical conductivity of GNP conductive ink is sheet resistivity. It was performed using JANDEL In-Lane Four-point Probe with 1 mm distance between each probe by referring to ASTM F390 standard [10]. Sheet resistivity is suitable to examine the electrical conductivity of thin film as compared to bulk resistivity [11].

2.2.2. Mechanical Properties

For the investigation of mechanical properties, a nanoindentation test was performed using Dynamic Ultra Micro Hardness with three-sided pyramidal Berkovich diamond tip. The obtained parameters include maximum indenter penetration, maximum force, hardness, and elastic modulus. The hardness and elastic modulus were acquired by analyzing the unloading data according to ASTM E2546-15 standard [12].

2.2.3. Microstructure Properties

The microstructure properties were investigated by obtaining the surface roughness and microstructure images of the GNP ink layer surface. The surface roughness was measured using Shodensa GR3400 non-contact profilometer. This instrument produces measurement readings by detecting the reflected light produced by the profilometer. To capture the microstructure images of the ink layer surface, JEOL JSM-5050PLUS/LV Emission Scanning Electron Microscopy (SEM) at 5 kV of accelerating voltage was used.

3. RESULTS AND DISCUSSION

3.1. Analysis of Electrical Properties

For the electrical properties, the data for sheet resistivity are tabulated in Table 2 below. The average values were obtained for every evaluated point on the ink samples. These data are graphically illustrated in Figures 3 and 4 as means of interpreting them according to trend and comparison.

Table 2 Sheet resistivity for GNP ink

Sheet Resistivity (Ω/sq)									
Width (mm)	**Point**	**Pattern**	**Average**	**Pattern**	**Average**	**Pattern**	**Average**	**Pattern**	**Average**
1	1	Straight line	55,597.440	Curve	268,929.975	Square	135,473.445	Zigzag	69,441.675
	2		79,634.270		124,686.350		130,539.613		150,092.758
	3		79,469.587		175,319.500		157,319.608		71,370.200
2	1		454,695.375		737,077.000		631,907.200		196,585.300
	2		470,436.950		294,098.380		917,675.050		184,604.647
	3		383,554.350		712,855.750		342,459.600		319,851.467
3	1		261,700.750		403,746.200		180,434.850		1,007,824.450
	2		428,529.360		411,043.350		366,091.020		925,244.1117
	3		338,419.200		231,469.700		465,622.520		1,077,955.867

Figure 3 below shows the comparison of sheet resistivity for different patterns. Based on the results, the straight-line pattern produces the lowest average of sheet resistance for all three thicknesses ranges from 56 kΩ/sq to 470 kΩ/sq. It follows by curve pattern with 125 kΩ/sq to 737 kΩ/sq, square pattern with 130 kΩ/sq to 918 kΩ/sq, and zigzag pattern with 69 kΩ/sq to 1,077 kΩ/sq. Based on previous research [7,20], in general, the electrical conductivity performance of the material is inversely proportional to the length of the conducting path. It is because conductivity depends on the electron mobility in the conducting material. The longer

electrical circuit increases the possibility of the electron colliding with more ions and increases the resistance as mentioned in previous research.

For this study, the GNP ink pattern of straight-line has the shortest length and follows by zigzag, curve, and square. Theoretically, the sheet resistance increment should follow this sequence. But the results in Figure 3 exposes slightly different outcomes, in which the shape of the pattern has a greater influence on sheet resistivity than the length of the pattern. All the bends and corners of the pattern produce a greater effect at the boundary conditions, which causes the boundary to become thicker and loosen [21,22]. The pattern with sharp edges produces higher resistivity, which is shown by square and zigzag patterns. It is similar with the literature [21] that the accumulation of acute angle design of pattern produces the highest resistivity because the trapped solvent inside the formulation prevents the forming of continuous and conductive path networks. For the pattern with the most angles, which is the zigzag patterns, the increment of pattern thickness is proportional to the sheet resistivity. It is expected that the increase of thickness reduces the sheet resistivity by creating more network of conducting paths. For this ink pattern, the existence of pores filled by the liquid solvent causes the nonuniform array of particles. It shows the similar findings as in [23]. As a result, it increases the sheet resistivity of the ink pattern. For the other patterns, the lowest sheet resistivity is at 1 mm of thickness and the highest sheet resistivity is at 2 mm of thickness.

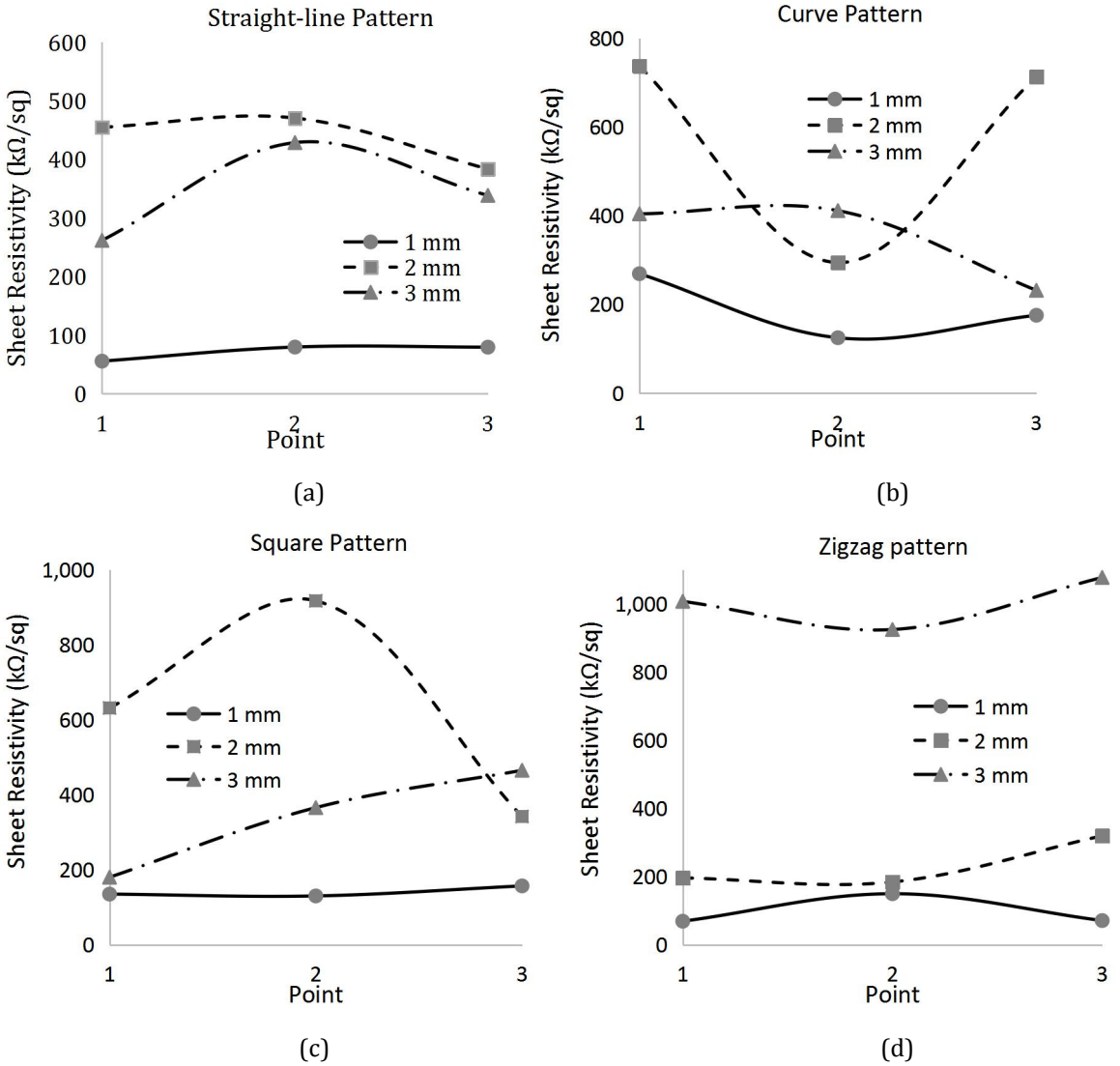

Figure 3. GNP ink sheet resistivity of different thickness for (a) straight-line, (b) curve, (c) square, and (d) zigzag patterns.

Figure 4 below shows the sheet resistivity of the ink for different sample thicknesses. It provides the comparison of sheet resistivity of different patterns with the same thickness. For the 1 mm thickness, the straight-line pattern shows the lowest sheet resistivity with the average value of 72 kΩ/sq and follows by zigzag with 97 kΩ/sq, square with 141 kΩ/sq, and curve with 190 kΩ/sq. It follows the sequence of the incremental length of the ink pattern with the shortest length produces the lowest sheet resistivity and vice versa. It is because the shortest ink pattern produces the least probability of the electron mobility to encounter other ions and causes resistance as mentioned in [20]. The measurements at Point 1 show a huge disparity, especially for the curve pattern. This is because of the defects due to the sample preparation procedure as shown in the morphological image in Figure 6, which illustrates the presence of inconsistent clumps. Similar findings were obtained by past researchers [24]. The disparity of data improves at the measurement of Point 2. It follows the incremental of sheet resistivity according to the length of the ink pattern. At Point 3, with the effect of pattern shape as described in the previous sub-chapter, the sheet resistivity trend is also changing.

For the thickness of 2 mm, the overall sheet resistance increases as compared to the thickness of 1 mm. Theoretically, the increase of pattern thickness increases the cross-sectional area of the conductive path. Consequently, it improves the electrical conductivity performance. But the results show different order. The incremental sequence changes starting with a zigzag pattern with the value of 234 kΩ/sq and follows by straight-line with 436 kΩ/sq, curve with 581 kΩ/sq, and square with 631 kΩ/sq. The main contributing factor is the composition of ink due to ink formulation, which will be further discussed in the morphological analysis.

Then, for a thickness of 3 mm, the incremental sequence of sheet resistivity is changing again. The pattern with the lowest average sheet resistivity is the square pattern with the value of 337 kΩ/sq and follows with straight-line with 343 kΩ/sq, curve with 348 kΩ/sq, and zigzag with 1.077 kΩ/sq. The patterns of square, straight-line, and curve show close dispersion of data. But the zigzag pattern produces the average sheet resistivity triple the values as the other patterns. With the increase of pattern thickness, the shape of the pattern produces greater influence as opposed to the increase of conductive path cross-sectional area. It conforms the findings in the literature [21] .

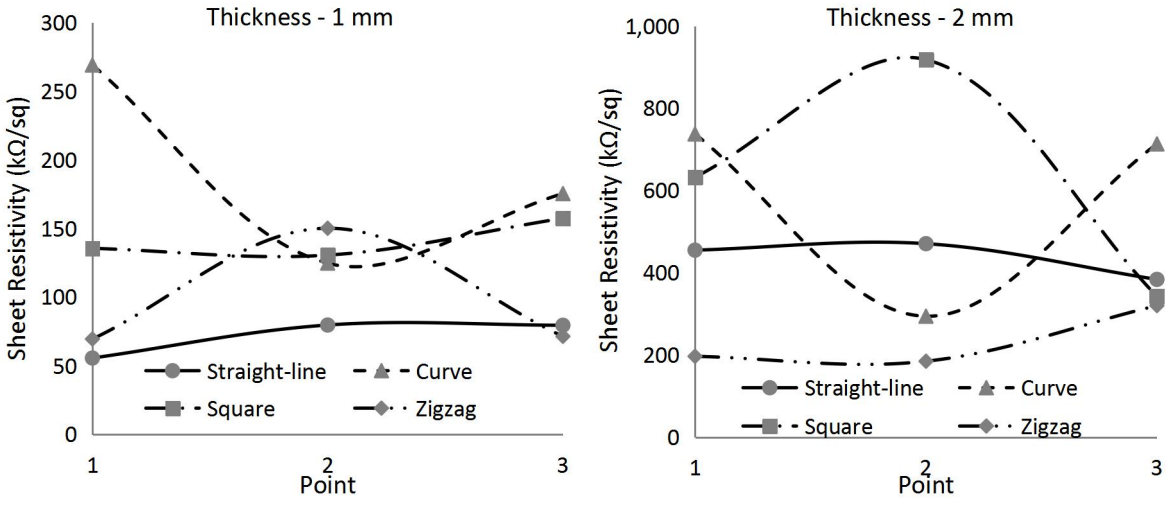

(a) (b)

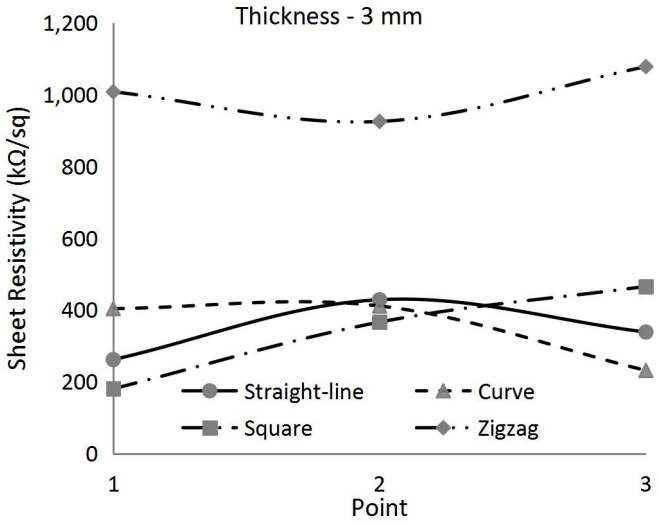

(c)

Figure 4. Comparison of GNP ink sheet resistivity of different patterns for (a) 1 mm, (b) 2 mm and (c) 3 mm thicknesses.

3.2. Analysis of Mechanical Properties

The mechanical properties of the samples were evaluated by performing a nanoindentation test. Four properties were assessed, which are the maximum force, maximum depth, hardness, and elastic modulus. The experiment can only be performed on the samples with the thickness of 2 mm and 3 mm. For the samples of 1 mm thickness, the size is too sample for the indenter tip to penetrate the material and produce any reading. The obtained data are tabulated in Table 3 below. For each of the properties, the data is illustrated in Figure 4 to determine its trend and parameter correlation. According to the literature, the pattern and width of ink produce an effect on the mechanical properties of the ink [25].

Table 3 Nanoindentation Properties of GNP Ink

Width (mm)	Pattern	Nanoindentation Properties			
		Maximum Force, F_{max} (mN)	Maximum depth, h_{max} (µm)	Hardness, H_u (GPa)	Elastic Modulus, E_{it} (GPa)
2	Straight-line	6.030	9.967	1.072	221.069
	Curve	6.024	5.152	1.416	552.187
	Square	6.000	4.034	3.489	788.383
	Zigzag	5.989	6.609	1.193	172.375
3	Straight-line	5.667	4.813	2.193	408.714
	Curve	5.998	5.350	4.913	659.865
	Square	5.992	7.137	1.940	575.807
	Zigzag	5.991	6.297	1.312	273.405

For the analysis of mechanical properties, one of the most important contributing factors is the polymer matrix of the ink. It is mentioned in previous research [26], which can describe the behavior of all the mechanical properties of the GNP ink. For the maximum forces, all the

patterns with both thickness values show almost consistent measurement as shown in Figure 4 (a). They can reach the preset maximum force value of 6 mN. The only outlier is the data for the straight-line pattern of 3 mm of thickness, which recorded the maximum force value of 5.667 mN. Then, Figure 4 (b) shows the maximum penetration depth of the ink. The highest recorded penetration depth is for the ink thickness of 2 mm, straight-line pattern with the value of 9.967 µm. The lowest penetration depth is recorded for the ink thickness of 2 mm, square pattern with the value of 4.034 µm. Both of highest and lowest penetration depth values are obtained at different peak loads. It also indicates that the penetration of the indenter parameter is independent of the magnitude of the load that conforms with the results by [27].

The relationship of material hardness for different patterns with the ink thickness of 2 mm and 3 mm is shown in Figure 4 (c). For the thickness of 2 mm, the highest recorded hardness is for the square pattern with the value of 3.849 GPa and the lowest is for the straight-line pattern with the value of 1.072 GPa. While the thickness of 3 mm recorded the highest hardness of 4.913 GPa for the curve pattern and the lowest of 1.312 GPa for the zigzag pattern. The hardness behavior is corresponding to the maximum penetration depth because the maximum load was set to be constant. The increase of hardness is caused by the increase of carbon content. The increase in carbon content causes the increment of penetration depth, which is similar with the findings of past research [16].

For the elastic modulus, it shows the same trend as for the hardness. The maximum values of elastic modulus for both ink thicknesses were recorded at the same pattern as for the hardness. It shows the direct correlation between the hardness and elastic modulus. The maximum value for 2 mm of thickness is the square pattern with the value of 788.383 GPa and for the 3 mm of thickness is the curve pattern with the value of 659.865 GPa. Furthermore, both properties show noticeable high values for both curve and square patterns. It corresponds to the length of the ink samples and the shape of the pattern. This behavior affirms the finding by past research that the pattern and width affect the mechanical properties of conductive ink [25].

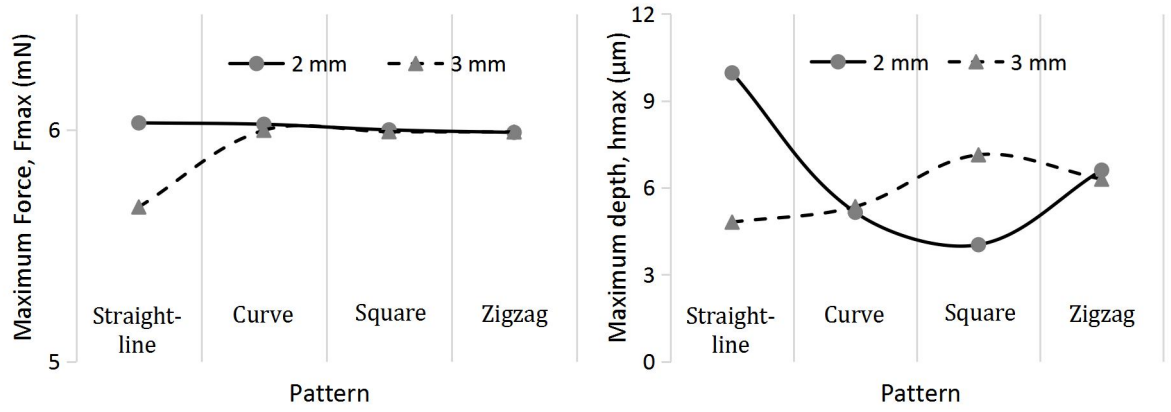

(a) (b)

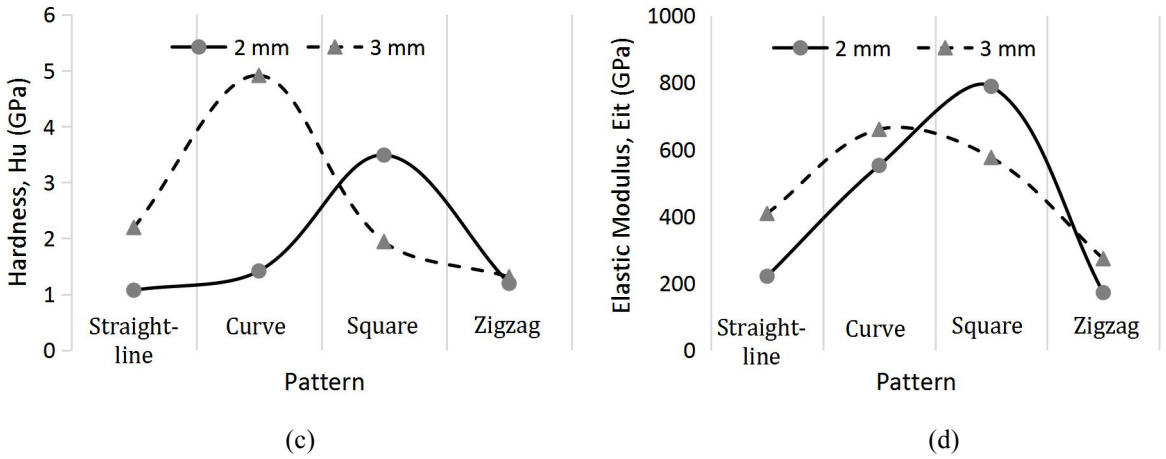

Figure 4. Mechanical properties of (a) maximum force, (b) elastic modulus, (c) hardness, and (d) elastic modulus of GNP ink at different thickness.

3.3. Analysis of Surface Roughness

The analysis for surface roughness was performed to show the comparison between the filler loading of GNP in the ink. The increase of surface roughness is proportional to the filler loading. At 10 %wt of filler loading, the surface roughness is 0.511µm and it increases exponentially when the filler loading was added to become 15 %wt with the value of 1.051µm. Then, the addition of filler loading shows a relatively constant rate of increment and achieves 1.543 µm at 35 %wt of filler loading. According to past research, the surface roughness is depending on the homogeneity of the composition.

The increment of GNP in the composition reduces the homogeneity and requires additional annealing time for the particles to reorientate and filling the gaps left by the evaporated solvent. Furthermore, the obtained data reveals that the surface roughness of the GNP conductive ink does affect the measurement of mechanical properties, which is also similar to the findings in the literature [15,28].

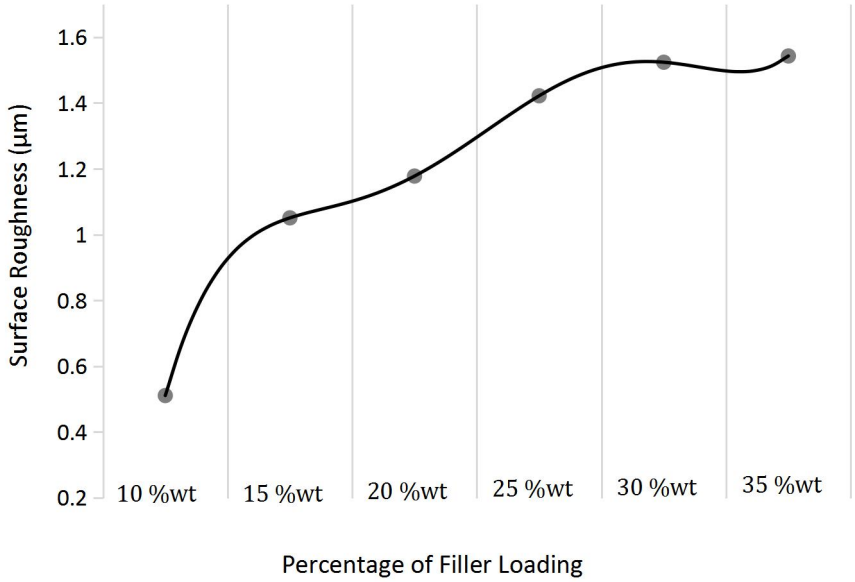

Figure 5. Surface roughness at different percentages of filler loading.

3.4. Analysis of Morphology

The ink layer surface of the GNP ink based on SEM images are illustrated in Figures 6 to 8 below. Figure 6 shows the morphology of 1 mm ink thickness for different types of patterns. Subsequently, Figures 7 and 8 show the images for the ink thickness of 2 mm and 3 mm, respectively.

For the images of ink thickness of 1 mm as in Figure 6, they show the apparent presence of bumps especially for curve pattern in Figure 6(b) and square pattern in Figure 6(c). The bump size up to 5 μm is shown for the curve pattern. It reduces the homogeneity of the composition, which reduces the density of conductive particle structure. This phenomenon is explained in the literature [29]. Because of that, it produces a high value of sheet resistivity of the GNP ink. For the straight-line and zigzag patterns, the surface microstructures show more well-distributed particles with less existence of ridges and creases. This indicates a good dispersion of GNP in the composition that forms proper conductive filler particle arrangement. It facilitates the electron tunneling effect, which increases the electrical conductivity behavior of the ink. This occurrence is also explained in the findings of previous research [7,28] The microstucture images ratify the sheet resistivity values of the ink as shown in Figure 4(a).

The SEM images in Figure 7 illustrate the ink layer surface microstructure for ink thickness of 2 mm. The zigzag pattern shows the most homogenous composition as compared to the other patterns with the well-distributed arrangement of particles. It follows by straight-line, curve, and square patterns. The homogenous composition produces less gap between the conductive particles, which allows the movement of electrons to flow between the particles. Thus, it increases the electrical conductivity of the composition as mentioned in [5]. The microstructure images in Figure 7 provide qualitative evidence of the sheet resistivity performance of the ink as shown in Figure 4 (b).

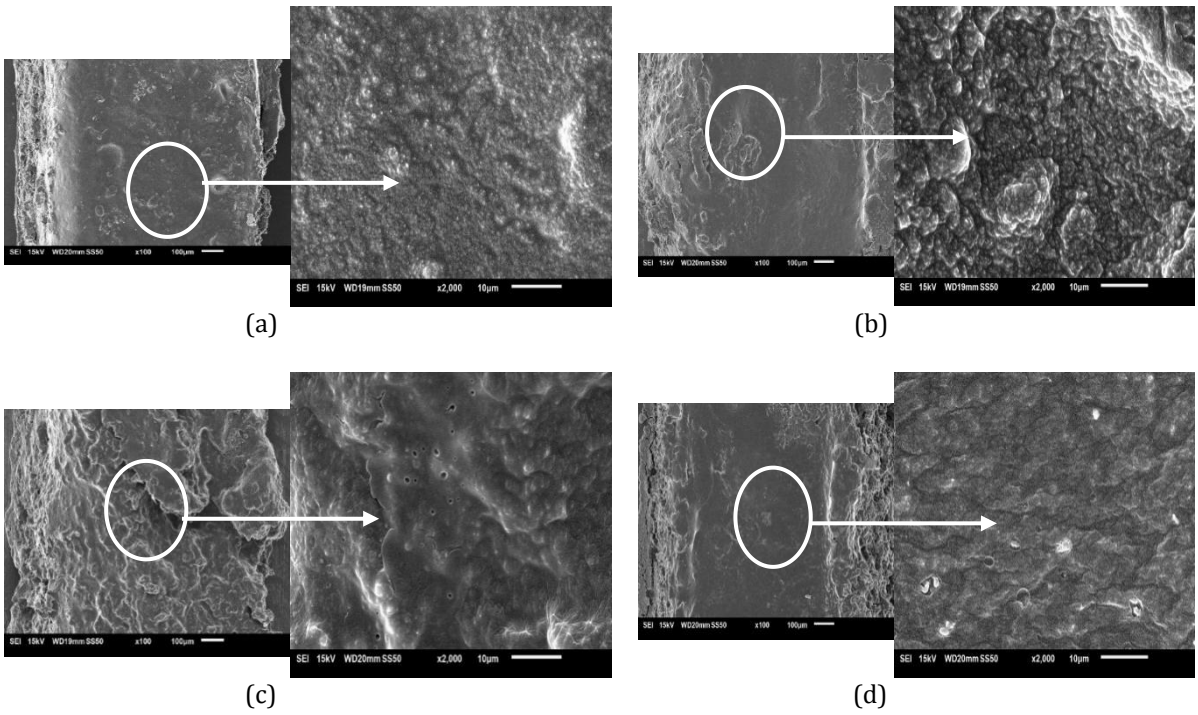

Figure 6. Surface microstructure images of GNP ink with 1 mm thickness for (a) straight-line, (b) curve, (c) square, and (d) zigzag patterns.

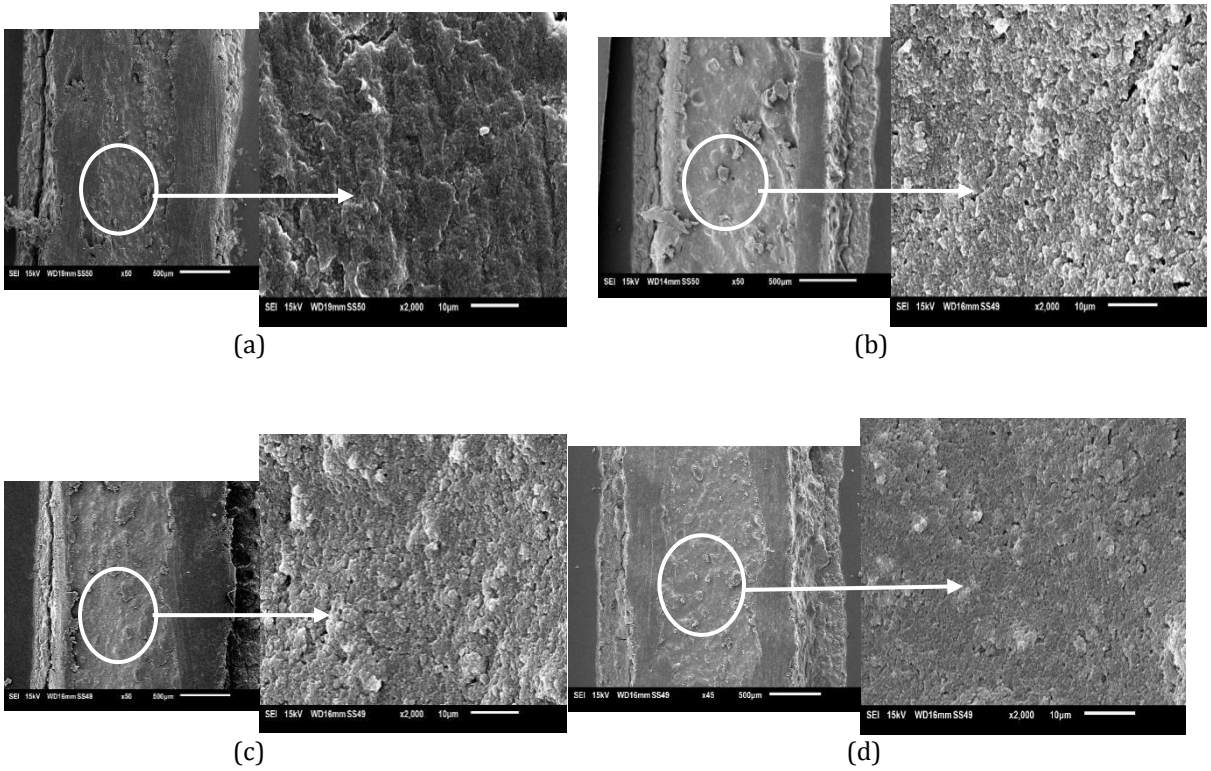

Figure 7. Surface microstructure images of GNP ink with 2 mm thickness for (a) straight-line, (b) curve, (c) square, and (d) zigzag patterns.

The microstructure SEM images for ink thickness of 3 mm are shown in Figure 8 below. The increase of ink thickness also increases the density of conductive filler in the composition. Thus, it enhances the homogeneity of the ink surface layer. Figure 8(c) shows the most homogenous composition and Figure 8 (d) shows the images with the most defects. These defects increase the particle gap that allows the movement of electrons, which are caused by the mismatch in crystallographic orientation or alignment of graphene lattice in various grains. Similar findings also explained by previous research [30] Thus, it reduces the electrical conductivity of the ink. For this study, ink with a thickness of 3 mm of zigzag pattern produces the highest sheet resistivity as shown in the microstructure image in Figure 8(d). All the microstructure images in Figure 8 are confirming the results of sheet resistivity obtained in Figure 4(c).

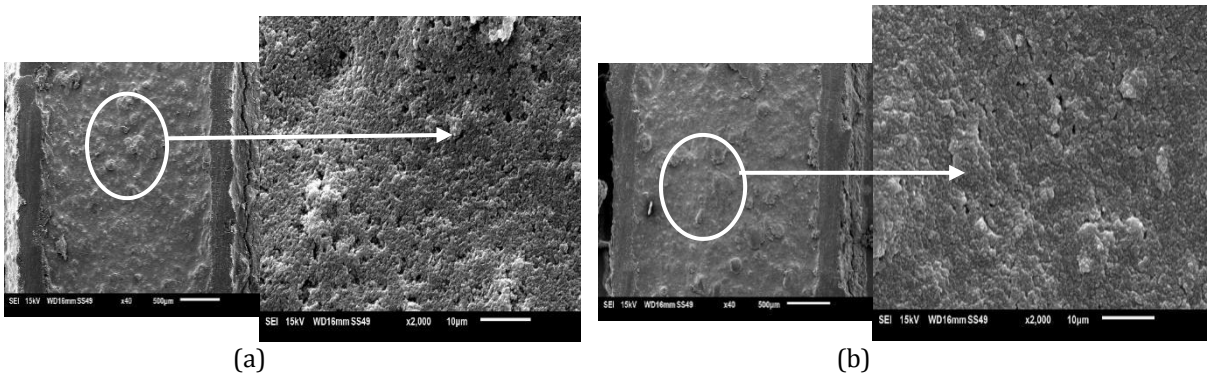

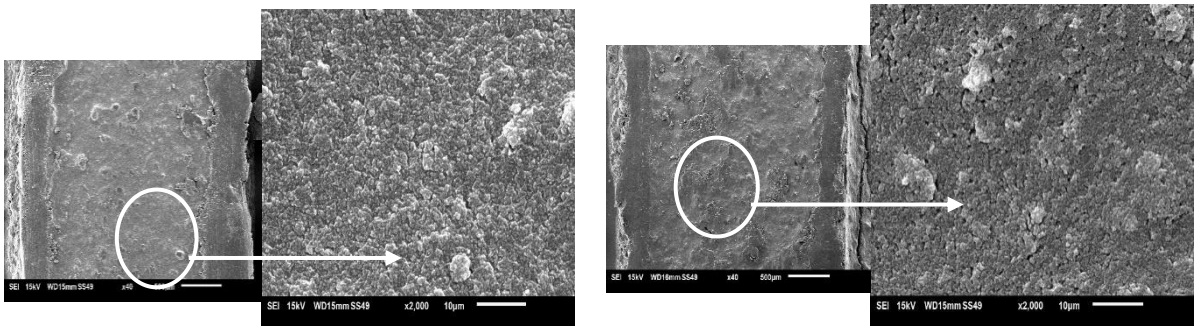

(c) (d)

Figure 8. Surface microstructure images of GNP ink with 3 mm thickness for (a) straight-line, (b) curve, (c) square, and (d) zigzag patterns.

4. CONCLUSION

This study investigates the electrical, mechanical, and morphological properties of different patterns of GNP conductive ink. The investigated parameter for the electrical property is the sheet resistivity, which shows that the zigzag pattern recorded the highest value of 1.077 kΩ/sq at the 3 mm of ink thickness. The sharp and acute angle of pattern produces a greater effect on boundary condition to become thicker and loosen, which prevents effective evaporation of solvent during the annealing process. It causes a high value of sheet resistivity. For mechanical properties, the maximum penetration depth trend corresponds to the hardness of the ink. The increase of the hardness also increases the penetration depth due to the increase of carbon content in the composition. The highest hardness for 2 mm thickness is the curve pattern and for 3 mm is the square pattern, with the values of 3.849 GPa and 4.913 GPa. Both maximum values show a direct correlation with the behavior of the elastic modulus of the ink. The maximum values of elastic modulus are recorded at the same ink pattern and thickness. The results show that the ink pattern and thickness produce a great effect on the mechanical properties of the ink. For the morphological analysis, the surface roughness and qualitative analysis using SEM images were performed. The surface roughness shows that the increase of GNP in the composition increases the surface roughness because it decreases the homogeneity of the mixture. The recorded SEM images of the ink layer microstructure surface show the direct correlation with the obtained sheet resistivity data. The samples that produce high sheet resistivity show the presence of bumps, creases, and defects on the ink layer surface. It affects the conductive particle arrangement in the composition and produces resistance for the electrons to flow. Based on the obtained data, the correlation between electrical, mechanical, and morphological properties can be established for the GNP conductive ink with various patterns and thicknesses. The GNP ink electrical conductivity performance can be further increased by utilizing a more suitable annealing process. By increasing the annealing temperature and time allow the conductive particle to have more energy to reorientate and form a homogenous arrangement. Furthermore, it permits more solvent to evaporate and reduce the gap between the conductive particles.

ACKNOWLEDGEMENTS

Special thanks to the Advanced Academia-Industry Collaboration Laboratory (AiCL) and Fakulti Kejuruteraan Mekanikal (FKM), Universiti Teknikal Malaysia Melaka (UTeM) for providing the laboratory facilities.

REFERENCES

[1] Y. Liu, W. Zhang, H. Yu, Z. Jing, Z. Song, and S. Wang, "A concise and antioxidative method to prepare copper conductive inks in a two-phase water/xylene system for printed electronics," *Chem. Phys. Lett.*, vol. **708**, (2018) pp.28–31.

[2] W. Li *et al.*, "The rise of conductive copper inks: challenges and perspectives," *Appl. Mater. Today*, vol. **18**, (2020) pp.100451.

[3] A. K. Ab Wahid *et al.*, "Driving monitoring system application with stretchable conductive inks: A review," *Int. J. Nanoelectron. Mater.*, vol. **13**, (2020) pp.327–346.

[4] Y. Chen *et al.*, "How is flexible electronics advancing neuroscience research?," *Biomaterials*, vol. **268**, no. December 2020, (2021) pp.120559.

[5] M. Mokhlis *et al.*, "Electrical Performances of Graphene Materials with Different Filler Loading for Future Super Conductor," *Def. S T Tech. Bull.*, vol. **12**, no. 2, (2019) pp.193–201.

[6] Z. Zhang, J. Sun, C. Lai, Q. Wang, and C. Hu, "High-yield ball-milling synthesis of extremely concentrated and highly conductive graphene nanoplatelet inks for rapid surface coating of diverse substrates," *Carbon N. Y.*, vol. **120**, (2017) pp.411–418.

[7] S. K. Kulkarni, *Nanotechnology - Principles and Practices 3rd ed (Springer, CP, 2015).pdf*. (2014).

[8] T. S. Tran, N. K. Dutta, and N. R. Choudhury, "Graphene inks for printed flexible electronics: Graphene dispersions, ink formulations, printing techniques and applications," *Adv. Colloid Interface Sci.*, vol. **261**, (2018) pp.41–61.

[9] Č. Žlebič *et al.*, "Electrical properties of inkjet printed graphene patterns on PET-based substrate," *Proc. Int. Spring Semin. Electron. Technol.*, vol. **2015**-Septe, (2015) pp.414–417.

[10] H. Saad, M. A. Salim, N. Azmmi Masripan, A. M. Saad, and F. Dai, "Nanoscale graphene nanoparticles conductive ink mechanical performance based on nanoindentation analysis," *Int. J. Nanoelectron. Mater.*, vol. **13**, (2020) pp.439–448.

[11] S. A. Peng *et al.*, "The sheet resistance of graphene under contact and its effect on the derived specific contact resistivity," *Carbon N. Y.*, vol. **82**, no. C, (2015) pp.500–505.

[12] J. Gong, Z. Peng, and H. Miao, "Analysis of the nanoindentation load-displacement curves measured on high-purity fine-grained alumina," *J. Eur. Ceram. Soc.*, vol. **25**, no. 5, (2005) pp.649–654.

[13] F. McGrath *et al.*, "Structural, optical, and electrical properties of silver gratings prepared by nanoimprint lithography of nanoparticle ink," *Appl. Surf. Sci.*, vol. **537**, no. August 2020, (2021) pp.147892.

[14] N. Ismail *et al.*, "The behaviour of graphene nanoplatelates thin film for high cyclic fatigue," *Int. J. Nanoelectron. Mater.*, vol. **13**, (2020) pp.305–314.

[15] M. Mokhlis, "A Study on Electrical and Mechanical Properties of Hybrid Ink Nanocomposite," Universiti Teknikal Malaysia Melaka, (2019).

[16] M. Mokhlis *et al.*, "Nanoindentation of graphene reinforced epoxy resin as a conductive ink for microelectronic packaging application," *Int. J. Nanoelectron. Mater.*, vol. **13,** (2020) pp.407–418.

[17] L. Liu, Z. Shen, X. Zhang, and H. Ma, "Highly conductive graphene/carbon black screen printing inks for flexible electronics," *J. Colloid Interface Sci.*, vol. **582**, (2021) pp.12–21.

[18] N. Ismail *et al.*, "Resistivity characterization for carbon based conductive nanocomposite on polyethylene terephthalate and thermoplastic polyurethane substrates," *Int. J. Nanoelectron. Mater.*, vol. **13**, no. Special Issue ISSTE 2019, (2020) pp.315–326.

[19] Y. Z. N. Htwe, M. K. Abdullah, and M. Mariatti, "Optimization of graphene conductive ink using solvent exchange techniques for flexible electronics applications," *Synth. Met.*, vol. **274**, no. December 2020, (2021) pp.116719.

[20] E. Yuliza, R. Murniati, A. Rajak, and M. Abdullah, "Effect of Particle Size on the Electrical Conductivity of Metallic Particles," no. January, (2014).

[21] J. Y. Park, W. J. Lee, B. S. Kwon, S. Y. Nam, and S. H. Choa, "Highly stretchable and

conductive conductors based on Ag flakes and polyester composites," *Microelectron. Eng.*, vol. **199**, no. January, (2018) pp.16–23.

[22] W. Zhang, M. Li, L. Gao, and X. Ban, "Surface characterization and electrical properties of spin- coated graphene conductive film," *16th Int. Conf. Electron. Packag. Technol. ICEPT 2015*, (2015) pp.56–59.

[23] K. Ryu, Y. J. Moon, K. Park, J. Y. Hwang, and S. J. Moon, "Electrical Property and Surface Morphology of Silver Nanoparticles After Thermal Sintering," *J. Electron. Mater.*, vol. **45**, no. 1, (2016) pp.312–321.

[24] H. A. D. Nguyen, N. Hoang, K. H. Shin, and S. Lee, "Improvement of surface roughness and conductivity by calendering process for printed electronics," *URAI 2011 - 2011 8th Int. Conf. Ubiquitous Robot. Ambient Intell.*, no. November, (2011) pp.685–687.

[25] J. M. Abu-Khalaf, L. Al-Ghussain, and A. Al-Halhouli, "Fabrication of stretchable circuits on polydimethylsiloxane (PDMS) pre-stretched substrates by inkjet printing silver nanoparticles," *Materials (Basel).*, vol. **11**, no. 12, (2018) pp.1–17.

[26] S. Merilampi, T. Laine-Ma, and P. Ruuskanen, "The characterization of electrically conductive silver ink patterns on flexible substrates," *Microelectron. Reliab.*, vol. **49**, no. 7, (2009) pp.782–790.

[27] H. Chen, L. xun Cai, and C. Li, "An elastic-plastic indentation model for different geometric indenters and its applications," *Mater. Today Commun.*, vol. **25**, no. June, (2020).

[28] T. Khan, M. S. Irfan, M. Ali, Y. Dong, S. Ramakrisna, and R. Umer, "Insights to low electrical percolation thresholds of carbon-based polypropylene nanocomposites," *Sci. Total Environ.*, (2019) pp.135907.

[29] A. Çelik *et al.*, *Carbon Nanotechnology Recent Developments in Chemistry, Physics, Material Science and Device Applications*, vol. **1**, no. 1, (2006).

[30] A. J. M. Giesbers *et al.*, "Defects, a challenge for graphene in flexible electronics," *Solid State Commun.*, vol. **229**, (2016) pp.49–526.